

# **Applied Journal of Physical Science**

Volume 6(4), pages 130-139, August 2025 Article Number: 0DBF5CBE2 ISSN: 2756-6684

https://doi.org/10.31248/AJPS2025.125 https://integrityresjournals.org/journal/AJPS

**Full Length Research** 

# Thermal, optical and passive radiation shielding efficiency of rice husk sourced glasses doped bismutite

Jibrin Suleiman Yaro<sup>1,2\*</sup>, Jamilu Ari Labaran<sup>1,3</sup>, Abdullahi Lawal<sup>4</sup>, Abdullahi Ibrahim Ode<sup>2</sup>, Iwa Samiya James<sup>2</sup> and Adamu Saidu<sup>4</sup>

<sup>1</sup>Department of Physics, Federal University of Lafia, Nasarawa State, Nigeria.

<sup>2</sup>Department of Physics, Federal University of Technology, Owerri, Imo State, Nigeria.

<sup>3</sup>Isa Mustapha Agwai Polytechnic, Lafia, Nasarawa State, Nigeria.

<sup>4</sup>Department of Chemistry, Federal University of Technology, Owerri, Imo State, Nigeria.

\*Corresponding author. Email: jibrinyarsuleiman@gmail.com

Copyright © 2025 Yaro et al. This article remains permanently open access under the terms of the <u>Creative Commons Attribution License 4.0</u>, which permits unrestricted use, distribution, and reproduction in any medium, provided the original work is properly cited.

Received 24th May 2025; Accepted 27th July 2025

**ABSTRACT:** Common shielding materials against highly penetrating radiations like X-rays and gamma photons are concrete and aggregates made of lead. On the other hand, concrete ages and turns opaque, and lead is costly and chemically dangerous. These and other factors have fuelled the ongoing quest for substitute radiation shielding materials. Mineral ores containing Rice Husk and bismuth ore have been generated by small-scale mining in Nigeria. Analysis of the ore found that 85.20% of the bismutite ( $Bi_2O_2CO_3$ ) and Rice Husk constituted 97.25% of silica. The new glass series was made from silica derived from Rice Husk and bismutite as dopants to alter the desired properties of the glass, with the empirical chemical formula  $[(SiO_2)_{20}(H_2BO_3)_{55}(Na_2CO_3)_{25}]_{100-x}(Bismutite)x$ , where  $1 \le x \ge 5$  wt.%. The glass series was created via the melt quenching process. Measurements of Physical, optical characteristics, X-ray attenuation, and thermal analysis of the glass systems were used to characterise the new glass. The glass system has refractive index values of 2.35-2.46. The produced glass was thermally stable. All glass samples were subjected to the X-Ray attenuation experiment of radiation shielding parameters, specifically the linear attenuation coefficient (LAC), mass attenuation coefficient (MAC), half value layer (HVL), and tenth value layer (TVL), at photon energies ranging from 40 to 80 kVp. The results indicate that the LAC and MAC of the glass samples decrease and increase as the photon energies increase from 40 to 80 kVp, while TVL and HVL increase and decrease as the photon energy increases (tube voltage).

Keywords: Bismutite, rice husk, optical, radiation shielding parameters, TGA, X-ray radiation.

### INTRODUCTION

In both therapeutic and diagnostic medicine, ionizing radiation has been employed more and more. However, ionizing radiation exposure can have negative effects on humans, which can be harmful to both patients and medical professionals. Therefore, in establishments that handle radiation sources, radiation protection regulations must be enforced. The management and use of radiation sources in hospitals and other businesses are governed by rules and regulations that have been promoted by nations all over the world (Acevedo-Del-Castillo *et al.*, 2021; Sekimoto and Katoh, 2015; Thomas and Symonds,

2016).

Radiation sickness, tumours, transmutation, and even death are some of the consequences of radiation exposure. It is clear that this is one of the most significant issues requiring the implementation of passive shields to reduce radiation exposure in order to safeguard hospital staff and patients. (Deepty *et al.*, 2019; Al-Buriahi *et al.*, 2020; Obaid *et al.*, 2018).

Radiation shielding is the science and practice of minimising damage to people and the environment from ionizing radiation. The biggest unknown when establishing nuclear power plants is radiation exposure, which calls for the use of robust radioisotopes, such as food preservation, tumour management, particle accelerator services, and diagnostic methods to stop radiation from harming staff and patients (Manohara et al., 2009; Peng et al., 20140; Rammah et al., 2021; Kolanoski and Wermes, 2020). To safeguard patients and staff, radiography institutions have incorporated a variety of safety equipment (Acevedo-Del-Castillo et al., 2021; Mostafa et al., 2020; IAEA, 2019; Sarachai et al., 2018).

Because of its high atomic number (Z), high density, high stability, and ease of processing, lead is one of the key shielding materials utilised in the creation of radiation shielding glass. However, lead is one of the main carcinogens, and its toxicity damages the ecosystem. Therefore, attempts are being made to substitute lead with other high atomic number metals in the manufacture of shielding glasses (Baptista Neto and Faria, 2014; Deepty et al., 2019; Sarachai et al., 2018; Singh et al., 2008). However, a thorough review of the literature showed that Rice husk and bismuthite-based glasses have not yet been thoroughly studied as possible substitutes for lead-based glasses in radiation shielding. Despite having a reduced effective density, these substitute materials are frequently effective shields (Gaikwad et al., 2018).

As a result, medical diagnostic and treatment procedures could be hazardous to health. Lead (Pb) based glasses are well-known and frequently used in analytical and medicinal applications due to their X-ray-defending capability to attenuate and absorb numerous varieties of photon energies (Kurudirek, 2017). High-density concrete can also be used to attenuate and absorb radiation; however, when concrete is exposed to moisture, it affects the strength and durability of the concrete, which may create a pathway for easy radiation exposure to a human being. Due to environmental concerns regarding the toxicity of lead concrete, other elements, such as Rice Husk (silica) and bismuth ore (bismutite) were used because of their low cost, durability, static, transparency, heat resistance, breakage resistance and chemical resistance to replace lead to produce radiation shielding glasses (Singh et al., 2008).

The objectives of this paper are to synthesise [(SiO<sub>2</sub>)<sub>20</sub>(H<sub>2</sub>BO<sub>3</sub>)<sub>55</sub>(Na<sub>2</sub>CO<sub>3</sub>)<sub>25</sub>]<sub>100-x</sub>(Bi<sub>2</sub>O<sub>2</sub>CO<sub>3</sub>)x, of the glass system, analyse the glass system's Physical, Thermal and Optical properties and to estimate the radiation shielding properties (HVL, LAC, MAC) of the glass system experimentally X-Ray. This work aims to fabricate, study the thermal, Optical and radiation shielding efficiency of the new glass series.

### THEORY BASIS

# The Linear Attenuation Coefficient μ (cm-1)

Linear attenuation coefficient  $(\mu)$  is the percentage of

photons extracted from a single energetic X-ray or gamma-ray beam per unit thickness of the material (Kara *et al.*, 2020). Beer-Lambert's law states that as the beam travels through the material, its intensity will be reduced.

$$I = l_o e^{-\mu x} \tag{1}$$

I = the intensity of photons transmitted across some distance X,  $I_0$  = the initial intensity of photons,  $\mu$ =the linear attenuation coefficient, X = the thickness of the material.

### Half Value Layer (HVL)

The half-value layer is defined as the thickness of the absorbing material that lowers the beam's intensity to half of its initial magnitude. The better the radiation shielding property in terms of thickness needed, the lower the HVL value (Kara et al., 2020). Half-value layer is calculated by the relation given below.

$$HVL = \ln \frac{2}{\mu} = \frac{0.693}{\mu} \tag{2}$$

Where  $\mu$  is the linear attenuation coefficient.

# **Tenth Value Layer (TVL)**

The half-value layer is the thickness of the absorbing material necessary to reduce the beam's intensity to a tenth of its initial value. The better the radiation shielding property in terms of thickness needed, the lower the TVL value (NDT, 2017). The tenth value layer is calculated by the relation given below.

$$TVL = ln \frac{10}{\mu} = \frac{2.303}{\mu} \tag{3}$$

# Mean Free Path (MFP)

The mean free path is the average distance a photon may travel through a substance before interacting (Sekimoto and Katoh, 2015). The relation has calculated the mean free path from the linear attenuation coefficient  $(\mu)$ .

$$MFP = \frac{1}{\mu} \tag{4}$$

### Glass fabrication

A series of glasses with the chemical formula  $[(SiO_2)_{20}(H_2BO_3)_{55}(Na_2CO_3)_{25}]_{100-x}(Bi_2O_2CO_3)x$ , where y is the weight percentage (x= 1, 2, 3, 4, 5%) of bismutite dopant in the glass matrix, was fabricated by using a melt-



**Figure 1.** Composition for X = 1,2,3,4 and 5 with empirical formula  $[(SiO_2)_{20}(H_2BO_3)_{55}(Na_2CO_3)_{25}]_{100-x}(Bi_2O_2CO_3)_x$  of the glass system.

quenching method. Powdered rice husk was the source of silica in this chemical composition.

The powdered samples were weighed based on the proportion in the empirical chemical formulas using an electronic balance by Adam PW 184 with serial number (180x0.0001g) AE437713. The weighed chemicals were then mixed and stirred for about 30 minutes in a clean alumina crucible to get a homogeneous mixture (Elmahroug et al., 2018; Gaikwad et al., 2018; Naseer et al., 2021). The mixture was then preheated at 400°C for 1 hour to remove moisture, particularly because of the hygroscopic B<sub>2</sub>O<sub>3</sub> (Abdul Aziz et al., 2015; Eevon et al., 2018). The preheated mixture was immediately transferred to another furnace for melting at 930°C for two hours. After melting, the molten glass was cast into a preheated mould before it was then annealed at 450°C for at least one hour in order to remove thermal stress and bubbles (Saad Aliyu et al., 2018; Naseer et al., 2021). Finally, the thickness of the glass was measured using a digital digimatic vernier calliper with model number HPM. After cutting and measuring the glasses, the glasses were then polished using a smooth surface silicon carbide paper (6cm x 2cm) to give the glasses a mirror finish (Naseer et al., 2021).

### X-ray radiation shielding measurement

The experimental measurement of X-ray radiation attenuation of the new glass systems was investigated to ascertain shielding effectiveness. The workroom was

equipped with a digital X-ray machine. Quality control was carried out to measure the output replicability, peak kilo voltage precision and peak kilo voltage replicability. The space distance between the glass samples and the X-ray tube was 45 cm, and the distance between the sources (tube voltage) to the detector window was kept at 100 cm. The exposure of the glasses was carried out at a fixed tube current of 20 mAs while the tube voltage was varied from 40, 50, 60, 70 and 80 kVp. A Geiger Mueller counter was used as the detector with a serial number GCA-07, model number GCA-07W, with an effective diameter of 1.5-2.0mg/cm<sup>2</sup>. The detector displays dose rates in millisievert per hour (mSv/hr), ranging from 0.0005 -10.0 mSv/hr (Suparta et al., 2014), (NDT, 2011). The setup of the photograph of X-ray radiation shielding properties measurement of the experiment is presented in Figure 2.

# Thermo Gravimetric Analysis (TGA) of the synthesised glasses

A thermal analytical technique called thermogravimetric analysis (TGA) is used to characterise substances based on their weight loss. It is a method for calculating a sample's weight in relation to temperature. With TGA, the sample is heated to a consistent temperature in a regulated setting, and the weight change is tracked over time. TGA provides a distinct picture of the analyte's makeup. Measuring weight growth or loss at a steady heating rate is the primary goal. Actually, the evaporation,

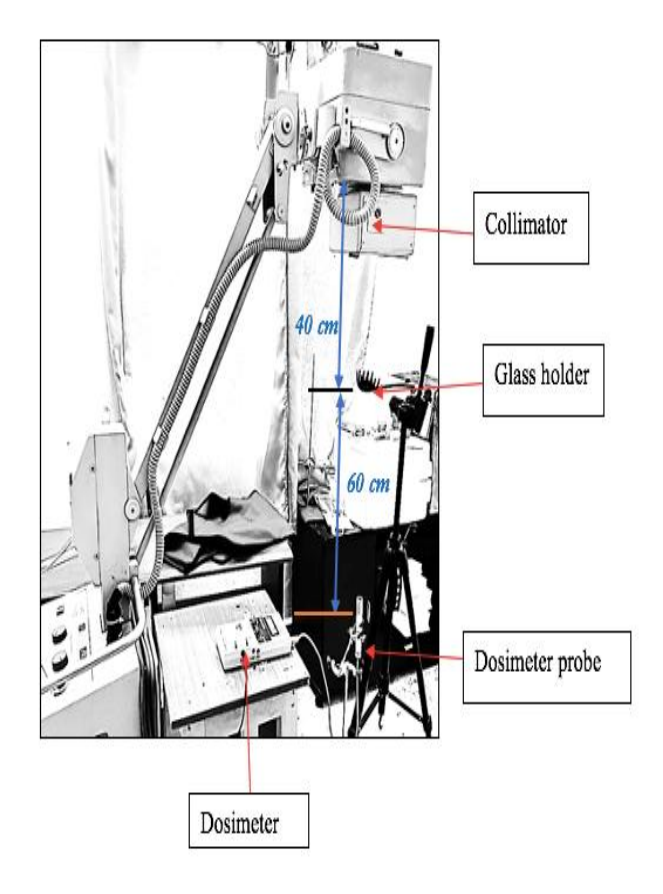


Figure 2. X-Ray experimental set-up.

oxidation, and breakdown of the analyte cause these weight variations.

The sample is put on an ultra-microbalance in a controlled environment in a thermal gravimetric analyser. Because it provides exact measurement using coupled thermocouples, the balance is regarded as the central component of TGA. The changes that take place during thermal examination are determined by the thermocouple (Abbas, 2023).

# Refractive index of the synthesised glasses

Refractive index is the measurement of how light propagates through a material. The higher the refractive index, the slower light travels through a material that changes its direction. It is a function of the material's electric permittivity and magnetic permeability, which also affects light speed (Saad Aliyu *et al.*, 2018). In glass sciences, the refractive index (n) is defined mathematically as a function of the optical energy band gap (E<sub>opt</sub>) as reported by (Eevon *et al.*, 2016);

$$n = \frac{n^2 - 1}{n^2 + 2} = 1 - \sqrt{\frac{E_{\text{opt}}}{20}}$$
 (5)

Where n is the refractive index,  $E_{opt}$  is the optical energy band gap of the glass system.

Figure 3 shows the UV-Visible absorption spectra plot of the glasses. The absorbance of the material against its wavelength, glass (GS) three (3) and five (5) has the highest absorbance while least absorbance was observed in glass (GS) four (4).

### **RESULTS AND DISCUSSION**

# Characterisations of bismutite and glass sand ores

Energy Dispersive X-ray Fluorescence (EDXRF) revealed the two ores contain ~60 wt% Bi and ~97.25wt.% Si, which denotes Bi-O, and the Bi ore contained C, O, V, Cu, Al and Si, while the Rice Husk metallic oxides are presented in Table 1. The EDXRF revealed that the rice husk contains 97.25% silica, which is needed as a glass former and some traces of metallic oxide impurities.

### Optical and thermal properties of the glasses

As the (Bi<sub>2</sub>(CO<sub>3</sub>)O<sub>2</sub>) concentration increased from 1 to 5

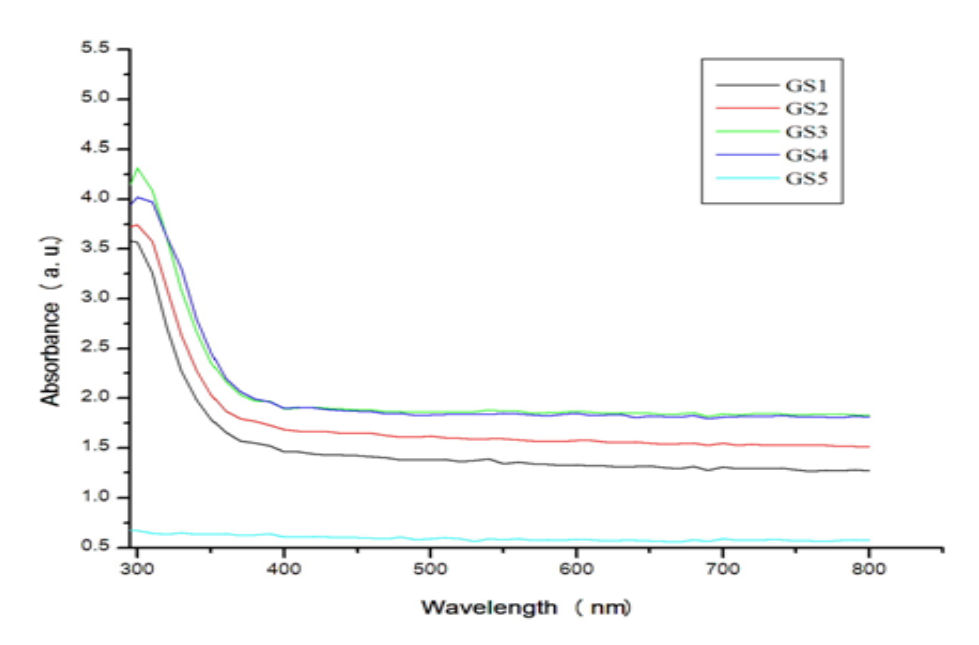


Figure 3. UV-Visible absorption spectra plot of the glasses.

**Table 1.** XRF analysis of extracted silica from rice husk.

Element (Oxide)	Amount /percentage (%)
Fe <sub>2</sub> O <sub>3</sub>	0.07
SiO <sub>2</sub>	97.25
AL <sub>2</sub> O <sub>3</sub>	1.80
MgO	0.53
CaO	0.11
K₂O	0.08
MnO	0.01
SO <sub>3</sub>	0.15

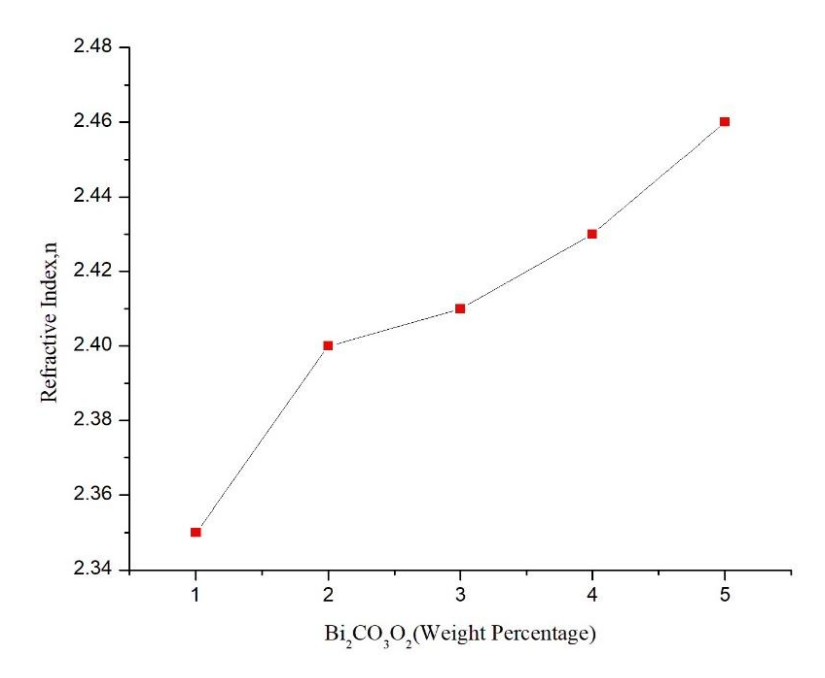
Table 2. Refractive Index of the glass system.

Bismutite = Y (wt. %)	Refractive Index (n)
5	2.35
10	2.40
15	2.41
20	2.43
25	2.46

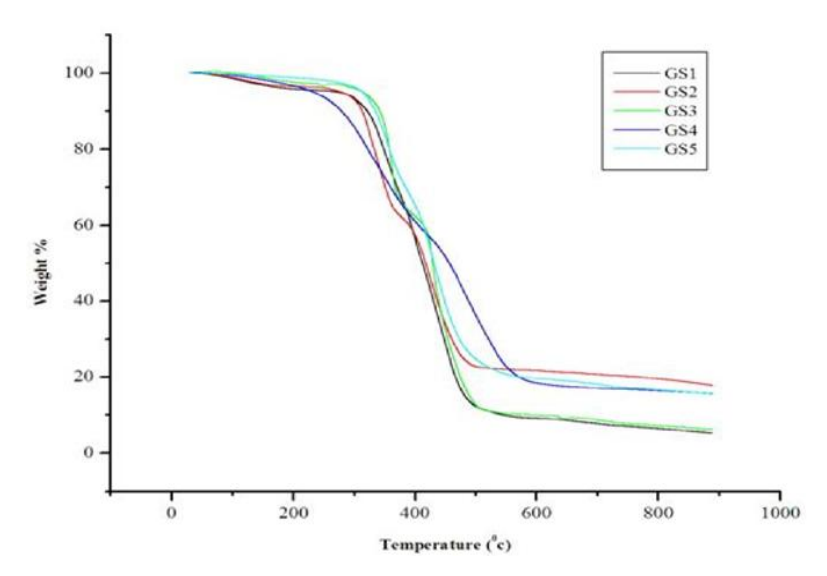
weight per cent of the fabricated glasses was investigated. The results of the refractive index (n) of the glasses were computed using Eq. 4 and are presented in Table 2. As observed, the refractive index increased from 2.35 to 2.46. The increase in the refractive index may be related to a change in the structural arrangements of the atoms in the glass network, as shown in Figure 4.

Figure 4 shows the refractive index of the glasses. The

results revealed that the refractive index of the fabricated glasses increased from 2.35 to 2.46. The increase in the refractive index may be related to a change in the structural arrangements of the atoms in the glass network that produces more NBOs, which increases the polarizability of the material through the increase in the NBOs produced. NBOs are more polarizable than bridging oxygen (BOs) (Eevon *et al.*, 2016).



**Figure 4.** Refractive Index of the Synthesized Glasses against weight percentage of Bismuth ore (Bismutite).



**Figure 5.** TGA for  $[(SiO_2)_{20}(H_2BO_3)_{55}(Na_2CO_3)_{25}]_{100-x}(Bi_2O_2CO_3)x$  of the glass system.

# Thermal analysis of the synthesised glasses

To determine how well the glasses worked for their thermal stability, thermal examination of the glass samples was done. Figure 5 displays the thermogram of the TGA result for the glass samples with a few various temperatures, such as the melting temperature (Tm), the initial temperature (Ti), and the final temperature (Tf). Additional

metrics, including mass weight change and glass forming ability Tgf that can be utilised to determine the useful application of the glass system. A greater resistance to thermal damage from the external environment is indicated by a higher Ti value (Abbas, 2023; Alam and Mohammad, 2021; Peng et al., 2014). According to Soltan et al. (2013), the glass's high temperature stability suggests a robust reserve of manifestation and nucleation

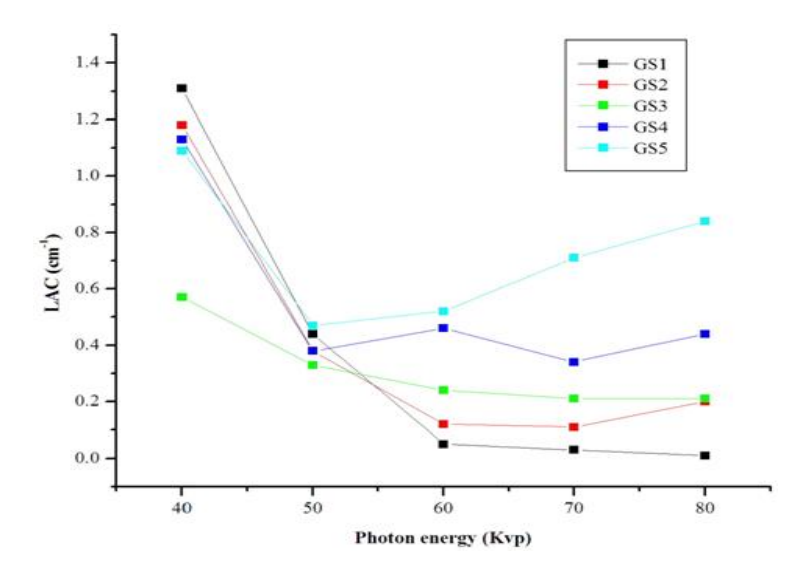


Figure 6. Linear attenuation coefficient of fabricated glass systems.

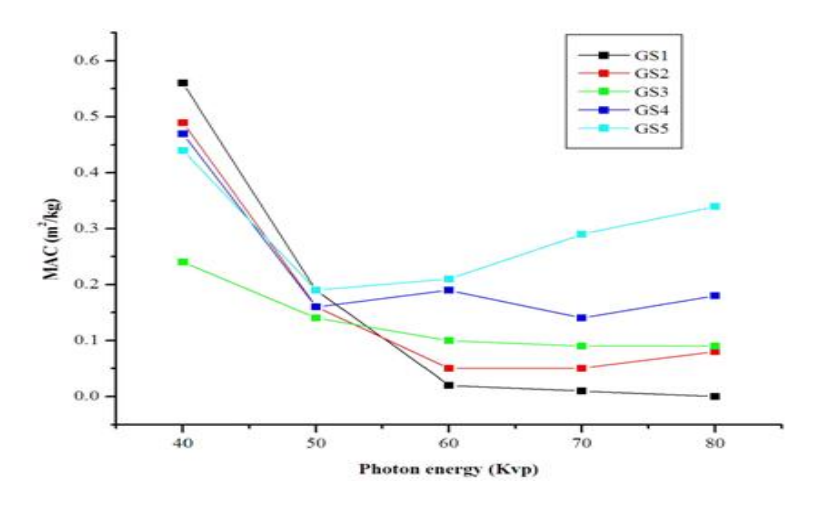


Figure 7. Mass Attenuation Coefficient of the fabricated glass.

within the glass structure. The glass system's thermal stability for different weight percentages, with temperatures ranging from 200 to 180°C, respectively, is observed. This indicates that the prepared glass system has a higher thermal stability and a more straightforward formation. According to Paz *et al.* (2016), glass that exhibits thermal stability above 100°C is both good for fibre drawing and stable against devitrification.

# X-Ray radiation shielding properties of glass samples

The glass samples produced were exposed to an X-ray beam in order to ascertain the radiation shielding ability of the glass. The result revealed that the LAC of all the glass

samples decreases and increases with the increase of photon energy (or tube voltage), ranging from 40 to 80 kVp. However, the results indicate that higher penetration of X-rays was observed at high photon energy.

Figure 6 shows that the higher the tube voltage, the higher the penetration. It was established that the glass samples at 1 wt.% of bismuth ore have the highest and the least linear attenuation coefficient values (LAC). Sarachai et al. (2018) reported that the glass samples fabricated are related to commercial lead glass.

Figure 7 shows that the mass attenuation coefficient of the glasses exhibited the same trend as that of LAC.

Figure 8 presents the HVL of the glass samples against photon energy (kvP). The results show that the half-value layer values of the glass samples at 40 and 60 kvP of GS1

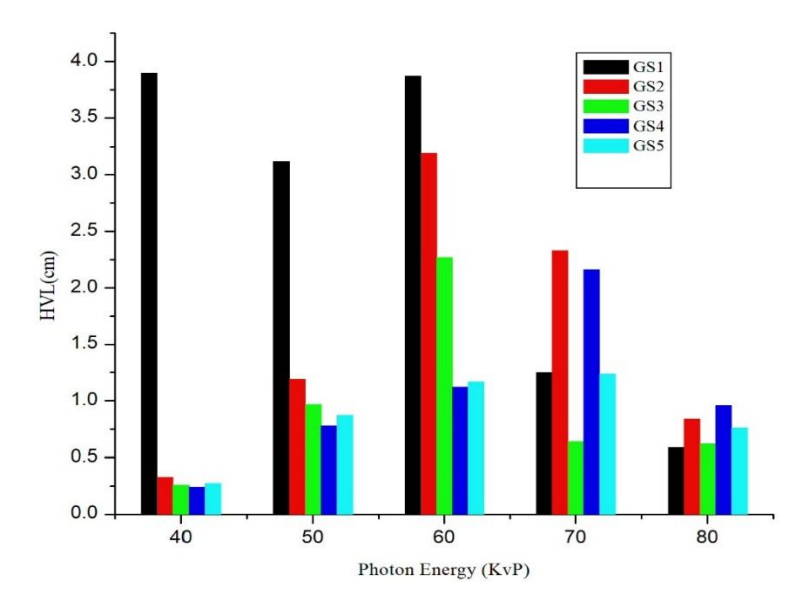


Figure 8. Half value layer of glass system.

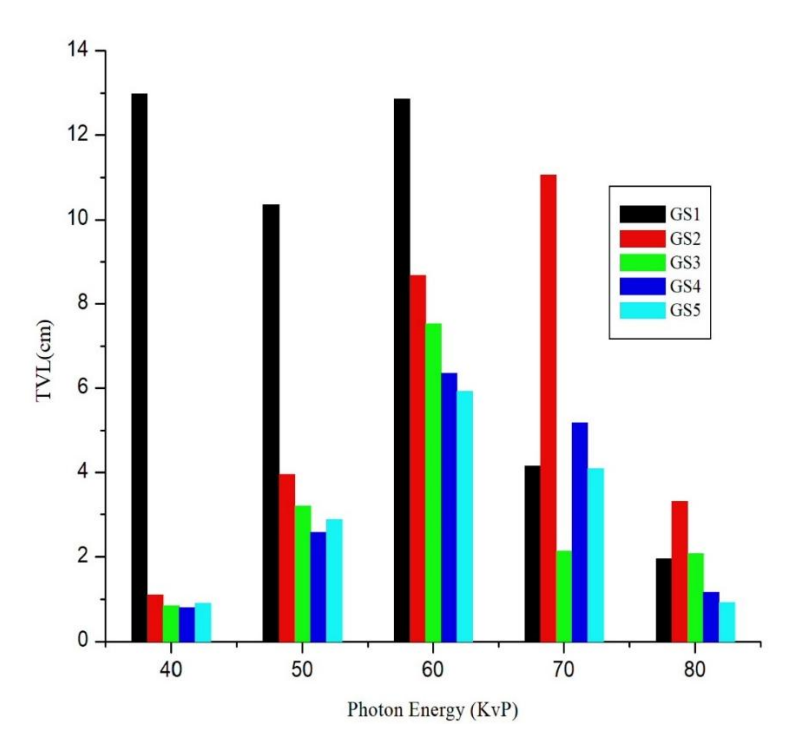


Figure 9. Tenth value layer of glass system.

are higher than all the samples, followed by GS2, while GS4 has the least half-value layer at 40KvP. This revealed that GS4 will attenuate better at 40 kvP.

Sarachai et al. (2018) reported the same as affirmation in Figure 8. It was established that the HVL values of the glass samples at 4 wt.% of Bismuth ore (Bismutite) are

lower than commercial lead glass. However, the glass samples produced (GS 2, 3, 4, and 5) attenuate better at 40kVp. It is shown that the innovative glasses have higher performance in radiation shielding.

The results illustrate that GS4 has the lowest tenth value layer at 40 kvP of photon energy, then GS3, while GS1 at

40 and 60kVp has the highest TVL. However, the figure revealed a similar trend to that of HVL. This might be as a result of k-edge absorptions by an increase in bismutites (Kaewjaeng *et al.*, 2023; Elsafi *et al.*, 2021).

### Conclusion

In this work, RH-sourced silica was extracted using acid leaching and calcinations and was used for the fabrication the empirical new glass with formula  $[(SiO_2)_{20}(H_2BO_3)_{55}(Na_2CO_3)_{25}]_{100-x}(Bi_2O_2CO_3)x, y = 1, 2, 3,$ 4, 5 weight percentage. The glass series was fabricated using the melt quenching method. The thermal, optical, and radiation shielding properties were investigated. The density of the glasses was found to increase with an increase in bismutite (Bi<sub>2</sub>O<sub>2</sub>CO<sub>3</sub>) content. The increase in density could be attributed to the high molecular weight of BiO<sub>2</sub>CO<sub>3</sub> (465.96 gmol<sup>-1</sup>). The glass system has a refractive index value between 2.35-2.46. The fabricated glasses are thermally stable.

The radiations shielding efficiency of the glasses was studied through the experimental measurement of MAC, LAC, TVL, and HVL within the five tube voltage (40, 50, 60, 70, and 80kVp) using mobile x-ray radiations source, there was noticeable decrease and increase in LAC and MAC values as photon energies increase from 40 to 80kVp while TVL and HVL increases and decreases as the photon energy increase (tube voltage). The addition of bismutite contents in the network improved the shielding efficiency of the glasses. It encourages disorderliness in the glass network, which causes X-rays, which have two orders of magnitude higher photon strength, to be attenuated more effectively by photoelectric absorption. These glasses are a desirable substitute for conventional radiation shielding materials due to their affordability and environmental advantages when made from rice husk and bismuth ore as raw components.

### **CONFLICT OF INTEREST**

The author states that there is no conflict of interest.

#### **REFERENCES**

- Abbas. B. (2023). *Thermogravimetric analysis (TGA)*. Definitive Guide. Pp. 214-223.
- Abdul Aziz, S. H., El-Mallawany, R., Badaron, S. S., Kamari, H. M., & Amin Matori, K. (2015). Optical properties of erbium zinc tellurite glass system. Advances in Materials Science and Engineering, 2015(1), 628954.
- Acevedo-Del-Castillo, A., Águila-Toledo, E., Maldonado-Magnere, S., & Aguilar-Bolados, H. (2021). A brief review on the high-energy electromagnetic radiation-shielding materials based on polymer nanocomposites. *International Journal of Molecular Sciences*, 22(16), 9079.

- Alam, S., & Chowdhury, M. A. (2021). Thermal gravimetric analysis of glass fiber reinforced composite for understanding the impact of copper oxide in relation to titanium oxide filler particles. Composites Theory and Practice, 21(1–2), 12–21.
- Al-Buriahi, M. S., Rashad, M., Alalawi, A., & Sayyed, M. I. (2020). Effect of Bi2O3 on mechanical features and radiation shielding properties of boro-tellurite glass system. *Ceramics International*, 46(10), 16452-16458.
- Baptista Neto, A. T., & Faria, L. O. (2014). Construction and Calibration of a multipurpose instrument to simultaneously measure dose, voltage and half-valuelayer in X-ray emission equipment. *Radiation Measurements*, 71, 178-182.
- Deepty, M., Srinivas, C., Kumar, E. R., Mohan, N. K., Prajapat, C. L., Rao, T. V. C., Meena, S. S., Verma, A. K., & Sastry, D. L. (2019). XRD, EDX, FTIR and ESR Spectroscopic Studies of Co-precipitated Mn–substituted Zn–ferrite nanoparticles. *Ceramics International*, 45(6), 8037-8044.
- Eevon, C., Halimah, M. K., Zakaria, A., Azurahanim, C. A. C., Azlan, M. N., & Faznny, M. F. (2016). Linear and nonlinear optical properties of Gd <sup>3+</sup> doped zinc borotellurite glasses for all-optical switching applications. *Results in Physics*, *6*, 761-766.
- Elmahroug, Y., Almatari, M., Dong, M., & Tekin, H. O. (2018). Investigation of radiation shielding properties for Bi<sub>2</sub>O<sub>3</sub> V<sub>2</sub>O<sub>5</sub> TeO<sub>2</sub> glass system using MCNP5 code. *Journal of Non-Crystalline Solids*, 499, 32-40.
- Elsafi, M., EL-Nahal, M. A., Sayyed, M. I., Saleh, I. H., & Abbas, M. I. (2021). Effect of bulk and nanoparticles Bi<sub>2</sub>O<sub>3</sub> on attenuation capability of radiation shielding glass. *Ceramics International*, *47*(14), 19651-19658.
- Gaikwad, D. K., Obaid, S. S., Sayyed, M. I., Bhosale, R. R., Awasarmol, V. V., Kumar, A., Shirsat, M. D., & Pawar, P. P. (2018). Comparative study of gamma ray shielding competence of WO3-TeO2-PbO glass system to different glasses and concretes. *Materials Chemistry and Physics*, 213, 508-517.
- IAEA (2019). Postgraduate Education Course in Radiation Protection and Safety of Radiation Sources: Standard Syllabus. *Training Course Series*, 18, 12-14.
- Kaewjaeng, S., Boonyu, K., Kim, H. J., Kaewkhao, J., & Kothan, S. (2020, October). Study on radiation shielding properties of glass samples doped with holmium. In AIP Conference Proceedings (Vol. 2279, No. 1, p. 060005). AIP Publishing LLC.
- Kara, U., Kavaz, E., Issa, S. A., Rashad, M., Susoy, G., Mostafa, A. M. A., Yildiz Yorgun, N., & Tekin, H. O. (2020). Optical, structural and nuclear radiation shielding properties of Li₂B₄O<sub>7</sub> glasses: effect of boron mineral additive. *Applied Physics A*, *126*(4), 261.
- Kolanoski, H., & Wermes, N. (2020). Introduction. In: Particle Detectors: Fundamentals and Applications. Oxford University Press.
- Kurudirek, M. (2017). Heavy Metal Borate Glasses: Potential use for Radiation Shielding. *Journal of Alloys and Compounds*, 727, 1227-1236.
- Manohara, S. R., Hanagodimath, S. M., & Gerward, L. (2009). Photon interaction and energy absorption in glass: A transparent gamma ray shield. *Journal of Nuclear Materials*, 393(3), 465-472.
- Mostafa, A. M. A., Zakaly, H. M. H., Pyshkina, M., Issa, S. A. M., Tekin, H. O., Sidek, H. A. A., Matori, K. A., & Zaid, M. H. M. (2020). Multi-objective optimization strategies for radiation

- shielding performance of BZBB glasses using Bi<sub>2</sub>O<sub>3</sub>: A FLUKA Monte Carlo code calculations. *Journal of Materials Research and Technology*, 9(6), 12335-12345.
- Naseer, K. A., Marimuthu, K., Mahmoud, K. A., & Sayyed, M. I. (2021). Impact of Bi<sub>2</sub>O<sub>3</sub> modifier concentration on barium-zincborate glasses: physical, structural, elastic, and radiation-shielding properties. *European Physical Journal Plus*, 136, 116.
- Obaid, S. S., Gaikwad, D. K., & Pawar, P. P. (2018). Determination of gamma ray shielding parameters of rocks and concrete. *Radiation Physics and Chemistry*, *144*, 356-360.
- Paz, E. C., Dias, J. D. M., Melo, G. H. A., Lodi, T. A., Carvalho, J. O., Façanha Filho, P. F., Barboza, M. J., Pedrochi, F., & Steimacher, A. (2016). Physical, thermal and structural properties of calcium borotellurite glass system. *Materials Chemistry and Physics*, 178, 133-138.
- Peng, S., Yang, F., Wu, L., Qi, Y., Zheng, S., Yin, D., Wang, X. & Zhou, Y. (2014). Multicolor upconversion emission and energy transfer mechanism in Er<sup>3+</sup>/Tm<sub>3</sub>+/Yb<sub>3</sub>+ codoped tellurite glasses. *Journal of Quantitative Spectroscopy and Radiative Transfer*, 147, 155-63.
- Rammah, Y. S., EL-Agawany, F. I., Gamal, A., Olarinoye, I. O., Ahmed, E. M., & Abuohaswa, A. S. (2021). Responsibility of Bi<sub>2</sub>O<sub>3</sub> content in photon, alpha, proton, fast and thermal neutron shielding capacity and elastic moduli of zinc/B<sub>2</sub>O<sub>3</sub>/Bi<sub>2</sub>O<sub>3</sub> glasses. *Journal of Inorganic and Organometallic Polymers and Materials*, 31(8), 3505-3524.
- Saad Aliyu, U., Mohamed Kamari, H., Muhammad Hamza, A., & Abdulla Awshah, A. (2018). The Structural, Physical and Optical Properties of Borotellurite Glasses Incorporated with Silica from Rice Husk. *Journal of Science and Mathematics Letters*, 6, 32-46.

- Sarachai, S., Chanthima, N., Sangwaranatee, N. W., Kothan, S., Kaewjaeng, S., Tungjai, M., Djamal, M., & Kaewkhao, J. (2018). Radiation shielding properties of BaO-ZnO-B<sub>2</sub>O<sub>3</sub> glass for X-ray room. *Key Engineering Materials*, 766, 88-93.
- Sekimoto, M., & Katoh, Y. (2015). Coloring characteristic of lead glass for X-ray irradiation. *New Journal of Glass and Ceramics*, *5*(3), 25-30.
- Singh, S., Kumar, A., Singh, D., Thind, K. S., & Mudahar, G. S. (2008). Barium–borate–flyash glasses: as radiation shielding materials. *Nuclear Instruments and Methods in Physics Research Section B: Beam Interactions with Materials and Atoms*, 266(1), 140-146.
- Soltan, A. S., Abu-Sehly, A. A. Joraid, A. A and. Alamri, S. N. (2013). The activation energy and fragility index of the glass transition in Se76Te21Sb3 chalcogenide glass. *Thermochimica Acta*, 574, 73-78.
- Suparta, G. B., Louk, A. C., Sam, N. H., & Wiguna, G. A. (2014, June). Quality performance of customized and low cost x-ray micro-digital radiography system. In *International Conference on Experimental Mechanics 2013 and Twelfth Asian Conference on Experimental Mechanics* (Vol. 9234, pp. 239-245). SPIE.
- Thomas, G. A., & Symonds, P. (2016). Radiation exposure and health effects Is it time to reassess the real consequences? *Clinical Oncology*, *28*(4), pp.231-236.